Cooperative Human-Robot Grasping With Extended Contact Patches

Sara Marullo, Maria Pozzi, Domenico Prattichizzo, and Monica Malvezzi

***Abstract*—Grasping large and heavy objects with a robot assistant is one of the most interesting scenarios in physical Human-Robot Interaction. Many solutions have been proposed in the last 40 years, focusing not only on human safety, but also on comfort and ergonomics. When carrying objects with large planar surfaces, classical contact models developed in robotic grasping cannot be used. This is why we conceived a contact model explicitly considering contact area properties and thus suitable to deal with grasps requiring large contact patches from the robot side. Together with the model, this work proposes a decentralized control strategy to implement cooperative object handling between humans and robots. Experimental results showed that the proposed method performs better than a simpler one, which does not account for contact patch properties. The control strategy is decentralized and needs minimal exteroceptive sensing (force/torque sensor at the robot wrist), so the proposed approach can easily be generalized to human-robot teams composed of more than two agents.**

***Index Terms*—Physical human-robot interaction, contact modeling, grasping.**

I. Introduction

COOPERATIVE manipulation between humans and robots is one of the most relevant examples of physical human-robot interaction (pHRI) [1]. Different scenarios have been tackled, from lifting of heavy objects [2], to transport of long or flexible objects [3]. The interaction is usually based either on impedance [4] or admittance [5] control schemes, where the controller parameters are often tuned exploiting observations of human-human interaction. Research works on human-robot cooperative manipulation focus on obtaining smooth human movements [6] and optimal load sharing [7] for a seamless and natural collaboration. Most of the times it is assumed that the robot is either tightly grasping the object with its gripper(s) [7], or that the object is attached to the robot through a universal joint [5]. So far, in the field of cooperative human-robot grasping, less focus has been put on deriving a model of the robot contacts taking into account the actual properties of the contacting surface. Also in the field of cooperative robot-robot manipulation, the common assumption is to consider the grasped object as firmly attached to each manipulator's end-effector (tightly grasped object) [8], and there are only a few works that explicitly model the contact points. In [9], for example, rotational/prismatic joints are used to model the rolling/sliding of the contacts.

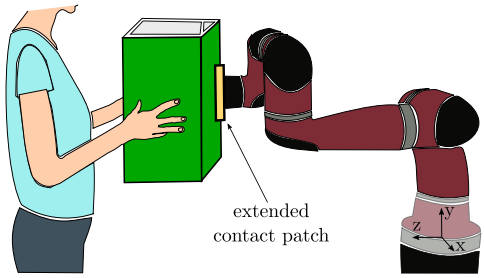

Fig. 1. Cooperative grasp between a human and a robot. The human guides the cooperative manipulation task and the robot keeps the grasp stable, avoiding sliding and rolling. The robot end-effector is equipped with a force sensor and a contacting plate ensuring an extended contact patch.

In this letter, we present a method to implement cooperative human-robot manipulation when the robot is not tightly grasping the object, but is contacting it with an extended patch. This set-up could be useful when carrying very large objects, as sketched in Fig. 1. In this scenario, the robot has the role of an additional finger contributing to the grasp stability through a decentralized control strategy based on the satisfaction of friction and pressure constraints. The robot contacting area is explicitly considered as an extended contact patch, through which all motions can be transmitted to the object, differently from the commonly used contact models for grasping tasks with multifingered hands.

Most of the literature on grasp analysis is based on models in which both the hand and the object are represented as rigid bodies, and contacts are identified in single points [10], [11]. These assumptions are at the basis of the main grasp quality measures [12], [13], and are also adopted in other applications, including the analysis of cooperative robot-robot and human-robot manipulation. Gupta *et al.*, for example, starting from the work conducted by Erdmann [14], assumed single point frictional contacts to plan carrying tasks with robots equipped with flat palms [15]. Contact models considering the resistance to torques about the contact normal direction (soft finger contact model [11]) have been exploited, instead, to simulate human

Manuscript received September 10, 2019; accepted January 29, 2020. Date of publication February 21, 2020; date of current version March 4, 2020. This letter was recommended for publication by Associate Editor M. J. Johnson and Editor A. M. Okamura upon evaluation of the reviewers' comments. This work was supported in part by the Progetto Prin 2017 "TIGHT: Tactile InteGration for Humans and arTificial systems," prot. 2017SB48FP, and by the IEEE RAS Technical Com-mittee on Haptics under the "Innovation in haptics" research programme. *(Corresponding author: Sara Marullo.)*

The authors are with the Department of Information Engineering and Mathematics, University of Siena, 53100 Siena, Italy, and also with the Department of Advanced Robotics, Istituto Italiano di Tecnologia, 16121 Genoa, Italy (e-mail: smarullo@diism.unisi.it; pozzi@diism.unisi.it; malvezzi@diism.unisi.it; prattichizzo@diism.unisi.it).

This letter has supplementary downloadable material available at http://ieeexplore.ieee.org, provided by the authors.

Digital Object Identifier 10.1109/LRA.2020.2975705

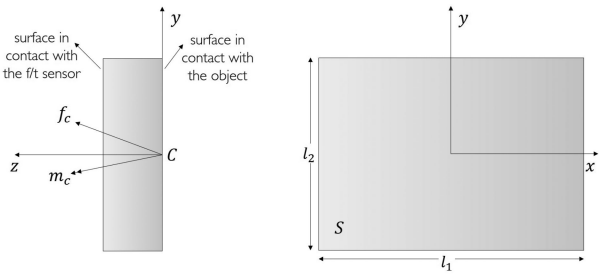

Fig. 2. Side and front view of the flat, rectangular plate attached to the force/torque sensor at the robot end-effector.

grasp capabilities [16], and to detect rotational slip with force and tactile sensors [17].

Extended contact patches have been explicitly modelled in many works on non-prehensile manipulation (e.g., planar pushing [18], planar sliding [19]), and, more recently, the concepts of *limit surface* [19] and *motion cone* [18] were used for planning prehensile in-hand manipulation actions through planar pushes [20]. Also the diffusion of soft robotic hands and their introduction in unstructured contexts [21], lead to an upgrade of the contact model, in order to consider contact patches with a finite and non-negligible area and local material deformation [22].

In this letter, we propose a contact model, namely the Extended Patch model, which explicitly takes into account an extended patch with known geometry. This model is an advance with respect to previous work as it not only considers tangential and normal friction limits, but also exploits the geometric properties of the patch to derive pressure constraints. Based on the Extended Patch model, a novel control scheme for cooperative human-robot grasping is introduced, in which the violation of friction constraints is translated into robot translational velocity commands, while the novel pressure constraints are used to derive angular velocities commands. This control strategy, called the Extended Patch method, was tested with 11 subjects. It resulted in a better human-robot team performance in terms of trajectory tracking accuracy and completion time, when compared to a method with a simplified control strategy not considering the contact patch properties, namely the Single Point method.

II. Contact Models

After some general definitions, here we briefly review the main contact models adopted in grasp analysis, and then introduce a model that considers a finite non-negligible contact area between robot end-effector and grasped object.

A. Definitions

Let us consider a plate whose surface goes in contact with the grasped object and is attached to a force/torque sensor at the robot end-effector, as in Fig. 1. For the sake of clarity, we assume that the contact area is flat and rectangular (Fig. 2). Let us define a contact reference frame whose origin C is in the centroid of the contact area, in which the $z-$axis is normal to the contact surface pointing to the plate, and x and y are aligned with plate's edges. When the plate is in contact with an object, it applies an equivalent contact wrench $\boldsymbol{\lambda}_c$ at the center of the contact patch C. $\boldsymbol{\lambda}_c$ collects the contact forces $\mathbf{f}_c$ and moments $\mathbf{m}_c$ in C: $\boldsymbol{\lambda}_c = [\mathbf{f}_c^T, \mathbf{m}_c^T]^T$, and it is balanced by the resultant of the tangential stresses and normal pressures applied to the plate. In each infinitesimal area dS of the contact patch there are a normal pressure $p(x, y)$ and two tangential stress components τ_x and τ_y. The resultant force and moment related to p, τ_x and τ_y, that have to balance $\boldsymbol{\lambda}_c$, are:

$$f_{cx} = -\int_S \tau_x dS, \quad f_{cy} = -\int_S \tau_y dS, \quad f_{cz} = -\int_S p dS \tag{1}$$

$$m_{cx} = -\int_S py dS, \quad m_{cy} = \int_S px dS,$$
$$m_{cz} = -\int_S (-\tau_x y + \tau_y x) dS \tag{2}$$

In the following, we summarize how these components are related in case the plate is approximated with a point (see Section II-B) or in case all geometrical properties of the actual contacting area are explicitly taken into account (Section II-C).

B. Background

1) Single Point With Friction (or Hard Finger): This is one of the simplest contact models, often adopted in grasp analysis literature, and it can be applied when the contact area is relatively small and the materials of the contact surfaces are sufficiently hard. In this situation, the contact can be approximated as a point and the action that is exchanged can be approximated with a force applied at the contact point, i.e., $\boldsymbol{\lambda}_c = [\mathbf{f}_c^T, \mathbf{0}^T]^T$. This force can be represented as the sum of a normal $f_n = f_{cz}$ and a tangential $f_t = \sqrt{f_{cx}^2 + f_{cy}^2}$ component, that are related by the Coulomb's friction constraint, i.e., $f_t \leq \mu_s f_n$, where μ_s is the static friction coefficient. In other words, Coulomb's law of friction imposes that $\mathbf{f}_c \in FC$, where FC is the *friction cone:*

$$FC = \left\{ \mathbf{f}_c \in \Re^3 : f_n \geq 0, f_t \leq \mu_s f_n \right\}. \tag{3}$$

2) Soft Finger: As in the previous model, the theoretical contact patch is assumed to be a point, but in this case we consider the local deformation of the contact surface. The action exchanged at the contact surface is the resultant of the distributions of normal pressure and tangential stress. Beside the tangential force f_t, the tangential stress can also generate a moment component m_{cz}. Since tangential stress and normal pressure have to locally satisfy Coulomb's friction law, that is $\tau_t = \sqrt{\tau_x^2 + \tau_y^2} \leq \mu_s p$, there is also a constraint between m_{cz} and f_n, i.e., $m_{cz} \leq \mu_t f_n$ [16].

C. Extended Patch (EP) Model

Both the models described above are based on the hypothesis that, neglecting the local deformations, the contact can be approximated with a point. In other words, both the models deal with non-conformal contacts [23]. In many implementations, however, this hypothesis cannot be applied. In this letter, for instance, we consider a human and a robot that have to lift and move an object together: it is obviously better to assume that

the robot is touching the object with an extended contact patch, through which it can apply forces and torques in all directions, rather than it is supporting the grasp in a single point. In this way, intuitively, the grasp is more reliable, and the human can fully control the object pose, while a part of its weight is supported by the robot.

To better explain the contact model that we are proposing, we do two hypotheses that simplify computations: a) the contact is flat, and b) the contacting surfaces are made of linear elastic materials. If one or both these hypotheses are not satisfied, the main steps of the procedure that will be presented can be applied as well by properly specifying contact materials' constitutive relationships and by evaluating the integrals in Eq. (1) and Eq. (2) over the non-flat surface.

From our hypotheses, it follows that the pressure distribution must be linear in x and y:

$$p = p_0 + ax + by. \tag{4}$$

Otherwise, the contact between the surfaces would be lost after the deformation. The parameters p_0, a and b in (4) are constant values that depend on the contact wrench $\boldsymbol{\lambda}_c$ and the plate surface S:

$$f_{cz} = -\int_S (p_0 + ax + by)dS \tag{5}$$

$$m_{cx} = -\int_S (p_0 + ax + by)ydS \tag{6}$$

$$m_{cy} = \int_S (p_0 + ax + by)xdS. \tag{7}$$

We can express p_0, a and b as functions of f_{cz}, m_{cx}, and m_{cy} by solving the above equations. If we assume that the surface of the plate is rectangular, with sides l_1 and l_2, and we substitute the obtained p_0, a and b in (4), we get:

$$p = \frac{f_{cz}}{l_1 l_2} + \frac{3m_{cy}}{l_1^3 l_2}x + \frac{3m_{cx}}{l_1 l_2^3}y. \tag{8}$$

Eq. (8) shows that the pressure is the sum of three terms: the first one is the mean pressure, due to the application of a normal force on a surface, while the others are the contributions provided by the applied torques in x and y directions. These components vary according to the Cartesian position of a given point on the surface. So, for instance, if just a counterclockwise rotation about x-axis is considered, the higher is the y-coordinates of a point, the higher is the pressure in that point. If an additional counter-clockwise rotation about y-axis is considered, the highest value of the pressure is in the right upper corner of the plate, while the minimum is in the bottom left corner. This is coherent with what is expected by intuition about forces and torques applied to a rectangular plate surface.

In order for the flat contact to hold, the following constraints must be satisfied for any point on the plate:

$$p(x, y) > 0 \tag{9}$$

When $m_{cx} \neq 0$ and/or $m_{cy} \neq 0$, pressure distribution over the contact area will not be constant and will have a minimum $p_{\min}$ and maximum $p_{\max}$ value. Assuming a rectangular plate, since the pressure distribution is linear, the boundary values $p_{\min}$ and $p_{\max}$ will result in one of the corners or, in some limit cases (when $m_{cx} = 0$ or $m_{cy} = 0$) on one of the edges. To verify that the contact is present, it is therefore sufficient to verify that Eq. (9) is satisfied for all the plate corners.

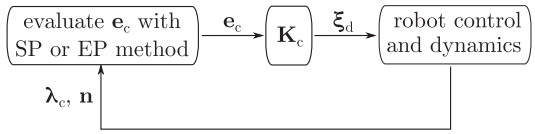

Fig. 3. Diagram of the force control with inner velocity loop.

Analogy with mechanics of structures: The introduced formulation has an interesting analogy with mechanics of structures analysis, and in particular in structures made of materials with a weak tensile strength, subject to compression and bending loading [24]. Let us consider the plate surface S (i.e., the plate with edges l_1 and l_2 in our case) as the equivalent structure cross section in our analogy, and f_{cz}, m_{cx} and m_{cy} its compression and bending loads. Such a loading condition is equivalent to an eccentric normal force with magnitude f_{cz}, applied in a point E on S surface whose coordinates are $x_E = \frac{m_{cy}}{f_{cz}}$, $y_E = -\frac{m_{cx}}{f_{cz}}$. E coordinates depend on the ratio between moment components and normal force. As the moment components increase, the distance between E and section centroid C increases. If the material is linear and elastic, the stress distribution resulting from this loading is planar and intersects the section plane in a line that is called central axis. Results from mechanics of structures show that is it possible to define a geometric place $\mathcal{C}$, called *central core*, of all points of application of the equivalent eccentric axial force, corresponding to neutral axis tangent to cross section contour. For any $E \in \mathcal{C}$ the neutral axis will fall outside section S and therefore the stress distribution will not change direction in all the section. Coming back to the extended patch contact problem, if $E \in \mathcal{C}$, $p(x, y) > 0$ in all the section. For a rectangular plate, the central core is a rhombus, centered in C with diagonals $l_1/3$ and $l_2/3$, respectively. □

III. Robot Control

The above introduced contact models are the basis of two force control algorithms that were implemented on a robotic arm to perform human-robot hybrid cooperative grasping. In both algorithms, the contact wrench $\boldsymbol{\lambda}_c$ and the normal direction $\mathbf{n}$ are inputs for the evaluation of force and torque correction terms denoted with $\mathbf{e}_f$ and $\mathbf{e}_m$, respectively. Indicating with $\mathbf{e}_c = [\mathbf{e}_f^T,\ \mathbf{e}_m^T]^T$ the complete correction vector, the reference robot speed value is then evaluated as $\boldsymbol{\xi}_d = \mathbf{K}_c\mathbf{e}_c$, where $\boldsymbol{\xi}_d = [\mathbf{v}_d^T,\ \boldsymbol{\omega}_d^T]^T$, $\mathbf{v}_d^T$ and $\boldsymbol{\omega}_d^T$ are the reference linear and angular velocities of the end-effector, respectively, and the subscript $_d$ indicates reference values. $\mathbf{K}_c = \mathrm{diag}[\mathbf{K}_f,\ \mathbf{K}_m]$ is a 6-dimensional diagonal matrix of the contact values transforming force and moment correction terms into translation and angular speed references, respectively. In other terms, in both the control algorithms, a force control scheme with an inner velocity loop is implemented, as shown in Fig. 3.

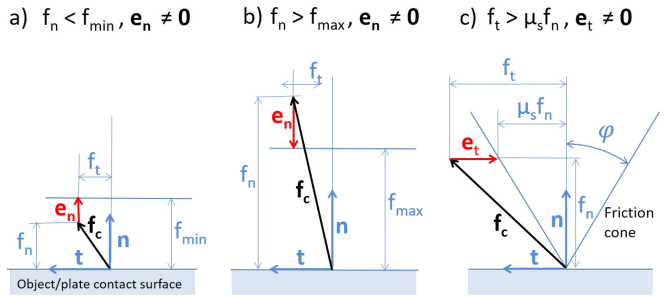

Fig. 4. Single Point method, evaluation of $\mathbf{e}_n$ and $\mathbf{e}_t$ in different cases. (a) $f_n < f_{\min}$, (b) $f_n > f_{\max}$, and (c) $f_t > \mu_s f_n$.

A. Single Point (SP) Method

This control algorithm is based on the single point with friction contact model. The robot is controlled so that: a) the normal component of the contact force f_n is bounded between two limits $f_{\min}$ and $f_{\max}$; b) the contact force $\mathbf{f}_c$ is inside the friction cone FC (Eq. (3)). SP contact model does not take into account moment components, however, since in our experimental implementation a flat end-effector was used, we had also to consider a moment correction term. Concerning this aspect, the control acted so to maintain the moment components as small as possible.

To accomplish these requirements, $\mathbf{e}_f$ and $\mathbf{e}_m$ are evaluated as detailed in Algorithm 1 and graphically represented in Fig. 4. The inputs of the algorithm are the current contact wrench $\boldsymbol{\lambda}_c$, the contact normal $\mathbf{n}$, $f_{\min}$, chosen to assure that $f_n > 0$ with a sufficient reliability, $f_{\max}$, taking into account the maximum force that the robot can apply and/or that can be applied to the object to avoid damages, and the friction coefficient μ_s.[1]

The force compensation term is the sum of two components: $\mathbf{e}_f = \mathbf{e}_n + \mathbf{e}_t$, where $\mathbf{e}_n$ is evaluated to assure that $f_{\min} < f_n < f_{\max}$, while $\mathbf{e}_t$ keeps f_t within Coulomb's friction limits. The contact moment component, $\mathbf{e}_m$, is an action opposite to $\mathbf{m}_c$ and is applied to keep its value as low as possible, i.e., $\mathbf{e}_m = -\mathbf{m}_c$.

B. Extended Patch (EP) Method

The Extended Patch contact model is the basis for the development of the second control algorithm. In this case, $\mathbf{e}_f$ is evaluated again as in Algorithm 1. The main difference with respect to SP control is in the evaluation of $\mathbf{e}_m = [e_{mx},\ e_{my},\ e_{mz}]$ term, that here explicitly takes into account the previously introduced contact properties and limits. e_{mz} action is applied if the normal component of contact moment exceeds torsional friction limits, i.e., if $m_{cz} > \mu_t f_{cz}$, and e_{mx} and e_{my} actions are applied if the equivalent pressure distribution $p(x, y) < 0$ in some parts of the contact patch.[1]

In the implementation proposed in this letter, p_i values are evaluated by Eq. (8) in the four plate corners P_i. Let $p_{\min}$ be their minimum value. If $p_{\min} < 0$, a corrective term $\mathbf{e}_{mb} = [e_{mx},\ e_{my},\ 0]$, is evaluated as $\mathbf{e}_{mb} = -k_{mb}|p_{\min}|\mathbf{b}$. Its magnitude is proportional to $|p_{\min}|$, and its direction is opposite to the tangential component of the contact moment, whose direction is defined by unit vector $\mathbf{b}$. Constant coefficient k_{mb}, depending on plate geometry, is necessary to transform the pressure in a torque reference. The evaluation of $\mathbf{e}_c$ components, and in particular of $\mathbf{e}_m$, is detailed in Algorithm 2.

[1]To account for a possibly inaccurate estimate of μ_s, we define $\mu_s = c_s \mu'_s$, where μ'_s is the estimated value and $c_s \in (0, 1]$ plays the role of *safety coefficient*. The same applies to μ_t.

Algorithm 1: Evaluation of $\mathbf{e}_c$, **SP** Method.

Input: $\mathbf{f}_c$, $\mathbf{m}_c$, $\mathbf{n}$, $f_{\min}$, $f_{\max}$, μ_s
Output: $\mathbf{e}_c$

loop
  $f_n \leftarrow \mathbf{f}_c \cdot \mathbf{n}$
  $\mathbf{t} \leftarrow \dfrac{(\mathbf{n} \times \mathbf{f}_c) \times \mathbf{n}}{|\mathbf{n} \times \mathbf{f}_c|}$
  $f_t \leftarrow \mathbf{f}_c \cdot \mathbf{t}$
  if $(f_n \leq f_{\min})$ **then**
    $\mathbf{e}_n \leftarrow (f_{\min} - f_n)\mathbf{n}$
  else if $(f_n \geq f_{\max})$ **then**
    $\mathbf{e}_n \leftarrow (f_{\max} - f_n)\mathbf{n}$
  else
    $\mathbf{e}_n \leftarrow \mathbf{0}$
  end if
  if $f_t \leq \mu_s f_n$ **then**
    $\mathbf{e}_t \leftarrow \mathbf{0}$
  else
    $\mathbf{e}_t \leftarrow f_t(1 - \frac{\mu_s f_n}{f_t})\mathbf{t}$
  end if
  $\mathbf{e}_f \leftarrow \mathbf{e}_n + \mathbf{e}_t$
  $\mathbf{e}_m \leftarrow -\mathbf{m}_c$
  $\mathbf{e}_c \leftarrow [\mathbf{e}_f^T,\ \mathbf{e}_m^T]^T$
  return $\mathbf{e}_c$
end loop

IV. Experiments

To validate the proposed contact model, experiments with a 7 DoFs collaborative robotic arm were performed. Skilled and non-skilled participants were involved. A *skilled* experimenter is a person familiar with collaborative robotics, and in particular with the cooperative manipulation setup used in the experiments. *Non-skilled* participants had never collaboratively grasped an object with a robot before.

Experiments were divided in two groups: *Characterization* (carried out by a skilled operator) and *Pick-and-Place* (carried out by 10 non-skilled operators). The method proposed in this letter, the Extended Patch method (EP), was compared to the Single Point approach (SP) in both cases. Experimenters were not informed about which method they were testing.

Characterization experiments were mainly aimed at evaluating the precision and overall functioning of the proposed control strategies in the most favourable conditions (i.e., user with consolidated experience with collaborative robots and with the specific experimental setup), and this is why they were performed by an expert operator. Pick-and-Place experiments,

Algorithm 2: Evaluation of $\mathbf{e}_c$, **EP** Method.

Input: $\mathbf{f}_c$, $\mathbf{m}_c$, $\mathbf{n}$, $f_{\min}$, $f_{\max}$, μ_s, μ_t, k_{mb}
Output: $\mathbf{e}_c$

loop
  $\mathbf{e}_f \leftarrow$ Algorithm 1
  $\mathbf{b} \leftarrow \dfrac{(\mathbf{n} \times \mathbf{m}_c) \times \mathbf{n}}{|\mathbf{n} \times \mathbf{m}_c|}$
  $p_i \leftarrow$ eval Eq. (8) at corners $P_i, i = 1 \cdots 4$
  $p_{\min} \leftarrow \min[p_1,\ p_2,\ p_3,\ p_4]$
  if $(p_{\min} > 0)$ **then**
    $\mathbf{e}_{mb} \leftarrow 0$
  else
    $\mathbf{e}_{mb} \leftarrow -k_{mb}|p_{\min}|\mathbf{b}$
  end if
  if $(m_{cz} < \mu_t f_n)$ **then**
    $\mathbf{e}_{mz} \leftarrow 0$
  else
    $\mathbf{e}_{mz} \leftarrow m_{cz}(1 - \frac{\mu_t f_n}{m_{cz}})\mathbf{n}$
  end if
  $\mathbf{e}_m \leftarrow \mathbf{e}_{mb} + \mathbf{e}_{mz}$
  $\mathbf{e}_c \leftarrow [\mathbf{e}_f^T,\ \mathbf{e}_m^T]^T$
  return $\mathbf{e}_c$
end loop

instead, were aimed at analysing user behaviour during a representative task that could be useful in industrial and domestic settings, and thus were performed by operators with different levels of experience.

In the performed experiments, we fixed the $\mathbf{K}_c$ gains as follows. The two methods used the same $\mathbf{K}_f$ ($\mathbf{K}_{f,SP} = \mathbf{K}_{f,EP} = diag(k_f, k_f, k_f)$), and two different $\mathbf{K}_m$ ($\mathbf{K}_{m,SP} = diag(k_{m,SP}, k_{m,SP}, k_{m,SP})$ and $\mathbf{K}_{m,EP} = diag(k_{m,EP}, k_{m,EP}, k_{m,EP})$) matrices, since the rotational correction of the two methods operates onto different quantities (torques for the SP method, pressures for the EP method). The gains k_f, $k_{m,SP}$, and $k_{m,EP}$ were chosen so to ensure safe robot reactions (too high gains would result into too high velocities) and acceptable performance in all motion directions.

To have a soft elastic contact between the box and the object, in both groups of experiments the object side closer to the robot was covered by a rubber layer. A Sawyer robotic arm (Rethink Robotics) equipped with an ATI Gamma force/torque sensor and a squared contacting plate at the end-effector was used for the experiments. Communication between the devices was implemented within the Robot Operating System (ROS).

A. Characterization Experiments

The operator is asked to move a box in cooperation with the robot, performing a simple trajectory for each trial, namely: i) a lateral translation of 50 cm along the x-axis (Fig. 1), ii) a vertical ascending translation of 50 cm along the y-axis, and iii) a translation of 50 cm towards the operator along the z-axis. The given task must be accomplished keeping as constant as possible Cartesian coordinates that are not explicitly involved in the task execution (e.g., in task ii) x and z must be perturbed as little as possible). However, since in collaborative robotics a special attention is dedicated to the human operator's comfort, the operator is asked to achieve a trade-off between comfort and assigned task. Each task was repeated 5 times with a 33 × 25 × 15 cm box weighting 0.5 kg.

Figs. 5 and 6 show the results obtained in terms of trajectories in task ii) using the the Single Point method and the Extended Patch method, respectively. For the other two tasks we obtained analogous results: a) for both methods the motion along the main task direction is almost linear, and b) the other two directions show a small variation between initial and final values when considering the EP method, whereas at least one of them varies considerably with the SP method. This is confirmed by the data reported in the right part of Table I.

To have an insight on how much the Cartesian coordinates are perturbed during the task execution, for each trial of each task, the difference between the initial and the final positions was recorded. The second to last column of Table I reports this position difference ($diff$) averaged over the 5 trials. Besides, for each trial of each task, the standard deviations along each motion direction were computed. The last column of Table I contains the worst case standard deviation ($maxstd$), i.e., the maximum computed value for the standard deviation achieved along each direction. When considering the secondary coordinates (i.e., the coordinates not explicitly involved in the task), the quantity $diff$ is always smaller for the EP method with respect to the SP one. For each task, for at least one coordinate, the ratio between the values obtained for the two methods is around one order of magnitude (see the x values for task ii)). While with Extended Patch method it is possible to well control all coordinates (with a maximum $diff$ of about 2 cm), with the Single Point approach human performance is less satisfactory. Similar conclusions can be drawn by looking at the values of $maxstd$.

In Table I, also averaged kinematic quantities and their standard deviations are reported, including the execution time (t), and the norms of force (f), torque (m) and velocity (linear (v) and angular (ω)) vectors.

B. Pick-and-Place Experiments

The operator is asked to move a box from a given start position to a given target position, placed 27 cm under it, 47 cm to the right (with respect to the human), and rotated of 35° about the vertical axis. The experimental setup is shown in Fig. 7. A box with size 36.5 × 34 × 11 cm and weight 0.4 kg was used. A total of 10 volunteers, 3 females and 7 males, aged between 26 and 54, participated to this experiment. None of them had previous experience of collaborative robotics and had ever tried the system. For this reason, they first had to accomplish a *training phase* and then a *test phase*. The training was composed of 2 trials with Extended Patch method and 2 trials with Single Point method, alternately proposed to the experimenter. After the training phase, one trial per method was performed for the test phase. Half of the participants first did the task with the EP method, while the others experimented first the SP method.

It should be remarked that the experimenters were not informed about which method was running, and they were not

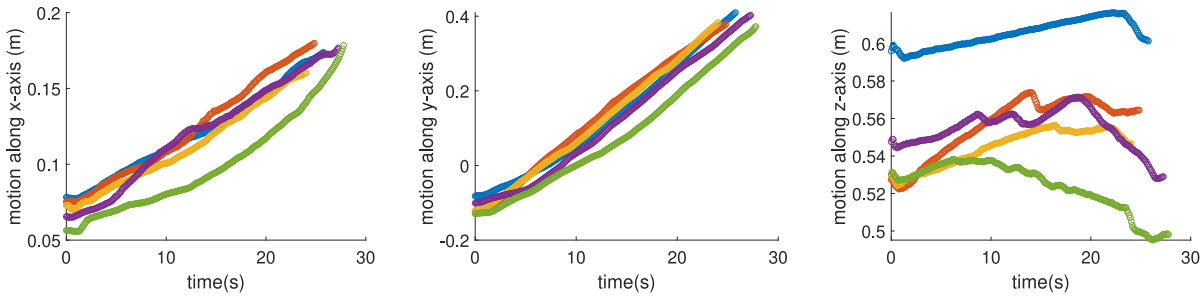

Fig. 5. Single Point method, Characterization experiments: results of 5 trials of task ii), i.e., object vertical motion. The motion in the y-axis is almost linear, similarly to Fig. 6. However, in this case, controlling the motion along x results to be more difficult than when using the Extended Patch method (see Table I).

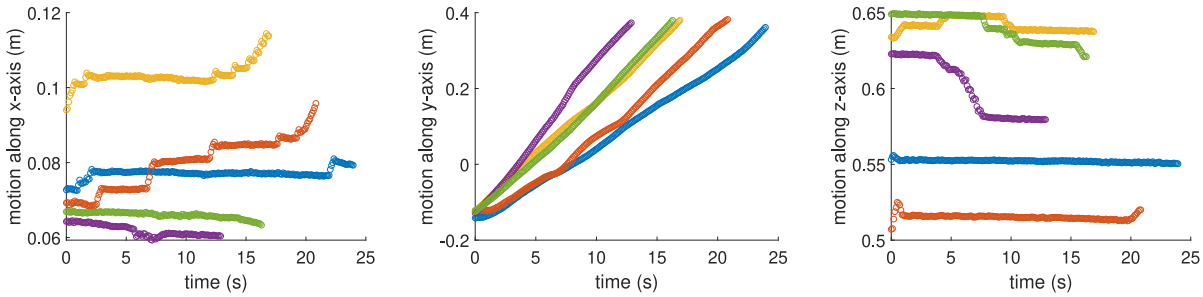

Fig. 6. Extended Patch method, Characterization experiments: results of 5 trials of task ii), i.e., object vertical motion. The motion in the y-axis is almost linear, and the other two directions are kept constant, or piecewise constant.

TABLE I

CHARACTERIZATION EXPERIMENTS. FOR EACH TASK, WE REPORT THE AVERAGE EXECUTION TIME (t), THE AVERAGE NORM OF FORCE (f) AND TORQUE (m), THE AVERAGE NORM OF THE LINEAR (v) AND ANGULAR (ω) VELOCITIES, THE AVERAGE DIFFERENCE ($diff$) BETWEEN INITIAL AND FINAL POSITION OF THE 5 TRIALS IN THE THREE DIRECTIONS, AND THE MAXIMUM RECORDED STANDARD DEVIATION BETWEEN THE POINTS OF THE TRAJECTORIES IN THE DIRECTIONS DIFFERENT FROM THE MAIN ONE ($maxstd$)

Test		t (s)	f (N)	m (Nm)	v (m/s)	ω (rad/s)	$diff$ (m)	$maxstd$ (m)
i) x-axis	SP	16.34 ($\pm$1.74)	8.66 ($\pm$0.43)	0.22 ($\pm$0.03)	0.033 ($\pm$0.003)	0.0016 ($\pm$0.0006)	[0.503, 0.067, 0.095]	[-, 0.037, 0.029]
	EP	18.77 ($\pm$1.80)	7.83 ($\pm$0.31)	0.21 ($\pm$0.03)	0.027 ($\pm$0.002)	0.0041 ($\pm$0.0017)	[0.504, 0.005, 0.021]	[-, 0.004, 0.015]
ii) y-axis	SP	25.93 ($\pm$1.57)	7.68 ($\pm$0.53)	0.26 ($\pm$0.02)	0.021 ($\pm$0.001)	0.0018 ($\pm$0.0003)	[0.104, 0.501, 0.022]	[0.034, -, 0.015]
	EP	18.16 ($\pm$4.28)	7.84 ($\pm$1.02)	0.25 ($\pm$0.02)	0.030 ($\pm$0.007)	0.0078 ($\pm$0.0039)	[0.012, 0.503, 0.018]	[0.007, -, 0.019]
iii) z-axis	SP	18.30 ($\pm$1.89)	2.29 ($\pm$0.27)	0.07 ($\pm$0.01)	0.028 ($\pm$0.003)	0.0003 ($\pm$0.0002)	[0.039, 0.072, 0.502]	[0.022, 0.029, -]
	EP	19.05 ($\pm$2.64)	2.48 ($\pm$0.34)	0.07 ($\pm$0.01)	0.027 ($\pm$0.003)	0.0027 ($\pm$0.0010)	[0.005, 0.010, 0.501]	[0.005, 0.007, -]

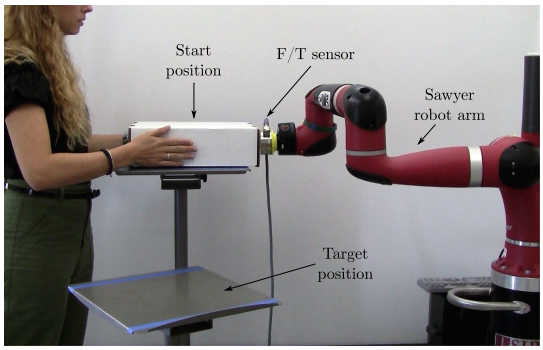

Fig. 7. Setup for the Pick-and-Place experiments.

even aware of the fact that their experiments were finalized to the comparison of two different approaches. None of the other participants was present while one of them was performing the experiment. Experimenters were told to move the box from the start to the target position with the aid of the robot and without loosing the contact with the robot. They were asked to accomplish the task as precisely (staying within the blue lines in Fig. 7) and as fast as possible.

Both phases of the experiments were analysed and the results are presented in the following.

1) Average Quantities: Data collected during the test phase have been processed so to obtain the average completion time and the average norms of the linear velocity and force. Results are reported in Table II which shows that while forces and velocities are similar for both methods, the average completion time decreases by $\sim$16% for the EP.

Three of the subjects, corresponding also to those that obtained the best performance in terms of completion time in the test phase, showed an interesting trend between the training and the test phase. The completion time of their experiments gradually decreased between the subsequent trials with the EP method and not with SP approach, as shown in Table III. This

TABLE II
PICK-AND-PLACE EXPERIMENTS. AVERAGE COMPLETION TIME, AVERAGE NORMS OF THE LINEAR VELOCITY AND FORCE DURING THE TEST PHASE OF THE PICK-AND-PLACE EXPERIMENTS

	SP	**EP**
t (s)	47.41	39.78
v (m/s)	0.018	0.02
f (N)	6.45	6.41

TABLE III
PICK-AND-PLACE EXPERIMENTS. COMPLETION TIME (S) FOR THE THREE OF THE SUBJECTS THAT OZNE OBTAINED THE BEST PERFORMANCE. FOR THEM, A GRADUAL REDUCTION OF THE COMPLETION TIME WHEN USING THE EXTENDED PATCH METHOD WAS OBSERVED. THE 1ST AND 2ND TRIALS BELONG TO THE TRAINING PHASE, THE 3RD ONE BELONGS TO THE TEST PHASE

Test		1st trial	2nd trial	3rd trial
Subject 1	SP	54.6	57.1	49.6
	EP	42.7	36.9	34.2
Subject 2	SP	41.7	33.8	41.1
	EP	47.2	34.9	26.8
Subject 3	SP	53.3	58.05	38.8
	EP	48.9	48.02	30.9

qualitative consideration highlights that the EP method fosters the familiarization with the task, even when participants are not yet skilled.

Another qualitative remark can be done when focusing on the data related to the 5 subjects that performed the first experiment of the training phase with the EP method and the second with the SP method. Although the trial with the EP method corresponded to their very first time doing a cooperative robotics experiment, all of them achieved a shorter completion time than that obtained with the SP method. The average difference was about 7.6 s.

By taking into account the first two trials of all the subjects, one done with EP and the other done with SP method, no matter the order in which the two methods were presented, 8 out of 10 experimenters achieved a shorter completion time with the EP method, with an average duration difference of 8.75 s. The same comparison for the test phase shows that the EP method allows a shorter completion time for 7 out of 10 subjects, with an average time difference between EP and SP of 11.6 s.

2) Task Precision and Contact Permanence: The proposed Pick-and-Place experiments involve more complex motions if compared with the motions required by the Characterization experiments, as the subjects were asked to perform a composition of translations and rotations.

Concerning task precision, participants were asked to precisely place the object in the target, clearly delimited, location. During the experimental trials, no relevant deviations were found with respect to the assigned location (average displacement $=$ 0.4 cm, average angle $= 6^\circ$).

Regarding contact permanence, the subjects were asked not to lose the contact between the box and the robot, and specifically to remain in contact with at least one corner of the contacting plate. During the test phase, with the SP method, an average angle between the end-effector surface and the box side of 30.1° about the plate $y - axis$ was measured. The same angle was just about 4.3° for the EP approach, that, however, also generated an average angle of 11.4° about the plate x-axis between the box and the plate.

3) Movement Smoothness: To have a comparative measurement of the movement smoothness achieved with the proposed methods, the SPARC (SPectral ARC length) index [25] has been computed for each experiment performed by the non-skilled subjects, and the average has then been retrieved. Calculations are based on the code available on GitHub.[2] The idea behind smoothness indices for a movement task is to analyse the derivatives of the position profile, so to highlight jerks. As suggested in [25], the data processing for the SPARC index related to a movement task with position measurements is related to velocities, since velocity "highlights intermittencies, and does not amplify noise as much as the other higher order derivatives". An average SPARC index was computed for each motion direction (x, y, z). The ratios between the corresponding SPARC indexes computed for the EP and the ones computed for the SP methods are 0.85, 0.99, and 1.02 for the three axes, respectively. These values do not highlight a relevant difference between the proposed approaches, since they are very close to 1. However, the same ratios computed for the subjects that obtained the best completion time (Table III) show a remarkable higher smoothness of the EP with respect to the SP method in the x and z axes (1.23, 1.07, 2.08).

V. DISCUSSION

Experiments reported in Section IV aimed at characterizing the performance achievable with the method presented in this letter, the Extended Patch method, and to provide a comparison with a simplest control strategy based on the Hard Finger contact model, the Single Point method.

During the Characterization experiments, based on performing pure translational motions and carried out by a skilled operator, average force, moment, linear velocity and completion time were found to be similar for the two methods (see Table I), showing that, as requested, the operator was naturally and comfortably performing the experiments with a similar effort. However, the Extended Patch method allowed to better control the object trajectory along the main direction of motion, keeping both the other directions almost constant or piecewise constant (see $diff$ and $maxstd$ in Table I, and Figs. 5, 6). Thus, the task was accomplished with more precision. Decreasing the unwanted displacement occurring in the secondary coordinates when using the Single Point method would have required more effort from the operator.

The Pick-and-Place experiments, involving a composition of translations and rotations, were carried out by non-skilled volunteers. All of them were able to precisely accomplish the task. The most relevant result obtained during these experiments is related to the contact permanence between the plate and the grasped object. For the Single Point method, at the end of the experiments, an average angle of 30.1° about the plate

[2][Online]. Available: http://github.com/siva82kb/SPARC

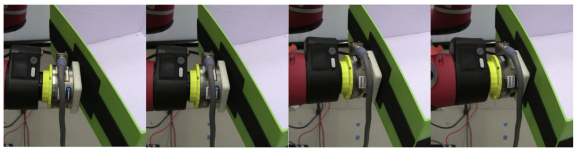

Fig. 8. Compensation of object rotation with the EP method.

y-axis appeared between the box and the plate. A much smaller detachment was measured with the Extended Patch method (4.3° about the y-axis, 11.4° about the x-axis). This implies that in the Single Point method, the operator has to choose whether to reduce the detachment actively, thus finishing the task with the box in a final wrong position, or to accomplish the task precisely, risking to lose the object. This would be particularly disadvantageous if the aid of the robot is necessary not only to stabilize the grasp but also to hold part of the weight of the object. A way to avoid this problem could be to finely tune the $\mathbf{K}_{m,SP}$ values (see Algorithm 1), which would require an inconvenient trial-and-error, task-dependent selection procedure. The small angular displacements obtained with the Extended Patch method are due to the fact that the robot does not have enough time to finish its rotational motion, as the experimenters are asked to complete the task as quickly as possible. However, the detachment could be avoided if subjects did slower motions. Subsequent frames of such situation are shown in Fig. 8, where the robot follows the object rotation thanks the Extended Patch method.

VI. Conclusion

We propose a new control strategy, the Extended Patch method, for human-robot cooperative manipulation based on a realistic contact model taking into account the actual shape of the contact region. This approach has been compared with a control strategy based on a contact model that is more similar to the most commonly used models in the literature and that does not consider the actual contact area properties. Our approach was validated in a cooperative manipulation setup and gave better results in terms of trajectory tracking and completion time. Preliminary, promising, results suggest also that it reduces users' learning time and increases movement smoothness, but these aspects will be better investigated in future work.

Future work will also focus on the application of the proposed method to cooperative manipulation between teams composed of more than one human and more than one robot, and to trimanual tasks, requiring the robot for stabilizing the grasp while the human guides the motion of the object with one hand and does other operations with the other.

References

[1] S. Haddadin and E. Croft, "Physical human–robot interaction," in *Springer Handbook of Robotics*, B. Siciliano and O. Khatib, Eds., Berlin, Germany: Springer, 2016, pp. 1835–1874.

[2] A. Mörtl, M. Lawitzky, A. Kucukyilmaz, M. Sezgin, C. Basdogan, and S. Hirche, "The role of roles: Physical cooperation between humans and robots," *Int. J. Robot. Res.*, vol. 31, no. 13, pp. 1656–1674, 2012.

[3] Y. Hayashibara, T. Takubo, Y. Sonoda, H. Arai, and K. Tanie, "Assist system for carrying a long object with a human-analysis of a human cooperative behavior in the vertical direction," in *Proc. IEEE/RSJ Int. Conf. Intell. Robots Syst. Human Environ. Friendly Robots with High Intell. Emotional Quotients*, 1999, vol. 2, pp. 695–700.

[4] R. Ikeura and H. Inooka, "Variable impedance control of a robot for cooperation with a human," in *Proc. IEEE Int. Conf. Robot. Autom.*, 1995, vol. 3, pp. 3097–3102.

[5] C. A. Parker and E. A. Croft, "Design & personalization of a cooperative carrying robot controller," in *Proc. IEEE Int. Conf. Robot. Autom.*, 2012, pp. 3916–3921.

[6] Y. Maeda, T. Hara, and T. Arai, "Human-robot cooperative manipulation with motion estimation," in *Proc. IEEE/RSJ Int. Conf. Intell. Robots Syst. Expanding Societal Role Robot. Next Millennium*, 2001, vol. 4, pp. 2240–2245.

[7] M. Lawitzky, A. Mörtl, and S. Hirche, "Load sharing in human-robot cooperative manipulation," in *Proc. 19th Int. Symp. Robot Human Interactive Commun.*, 2010, pp. 185–191.

[8] F. Caccavale and M. Uchiyama, "Cooperative manipulation," in *Springer Handbook of Robotics*, B. Siciliano and O. Khatib, Eds., Berlin, Germany: Springer, 2016, pp. 989–1006.

[9] P. Chiacchio, S. Chiaverini, and B. Siciliano, "Direct and inverse kinematics for coordinated motion tasks of a two-manipulator system," *J. Dyn. Syst., Meas., Control*, vol. 118, no. 4, pp. 691–697, 1996.

[10] A. Bicchi, "Hands for dextrous manipulation and robust grasping: A difficult road towards simplicity," *IEEE Trans. Robot. Autom.*, vol. 16, no. 6, pp. 652–662, Dec. 2000.

[11] D. Prattichizzo and J. C. Trinkle, "Grasping," in *Springer Handbook of Robotics*, B. Siciliano and O. Khatib, Eds., Berlin, Germany: Springer, 2016, pp. 955–988.

[12] M. Malvezzi and D. Prattichizzo, "Evaluation of grasp stiffness in underactuated compliant hands," in *Proc. IEEE Int. Conf. Robot. Autom.*, 2013, pp. 2074–2079.

[13] M. A. Roa and R. Suarez, "Grasp quality measures: Review and performance," *Auton. Robots*, vol. 38, no. 1, pp. 65–88, 2015.

[14] M. Erdmann, "An exploration of nonprehensile two-palm manipulation," *Int. J. Robot. Res.*, vol. 17, no. 5, pp. 485–503, 1998.

[15] A. Gupta and W. H. Huang, "A carrying task for nonprehensile mobile manipulators," in *Proc. IEEE/RSJ Int. Conf. Intell. Robots Syst.*, Oct. 2003, vol. 3, pp. 2896–2901.

[16] F. Barbagli, A. Frisoli, K. Salisbury, and M. Bergamasco, "Simulating human fingers: A soft finger proxy model and algorithm," in *Proc. 12th Int. Symp. Haptic Interfaces for Virtual Environ. Teleoperator Syst.*, 2004, pp. 9–17.

[17] C. Melchiorri, "Translational and rotational slip detection and control in robotic manipulation," *IFAC Proc. Volumes*, vol. 32, no. 2, pp. 647–652, 1999.

[18] M. T. Mason, "Mechanics and planning of manipulator pushing operations," *Int. J. Robot. Res.*, vol. 5, no. 3, pp. 53–71, 1986.

[19] S. Goyal, A. Ruina, and J. Papadopoulos, "Planar sliding with dry friction part 1. Limit surface and moment function," *Wear*, vol. 143, no. 2, pp. 307–330, 1991.

[20] N. C.-Dafle, R. Holladay, and A. Rodriguez, "Planar in-hand manipulation via motion cones," *Int. J. Robot. Res.*, vol. 39, nos. 2/3, pp. 163–182, 2019.

[21] R. Deimel, C. Eppner, J. A.-Ruiz, M. Maertens, and O. Brock, "Exploitation of environmental constraints in human and robotic grasping," *Robotics Research*. Springer, 2016, pp. 393–409.

[22] S. Dharbaneshwer, S. J. Subramanian, and K. Kohlhoff, "Robotic grasp analysis using deformable solid mechanics," *Meccanica*, vol. 54, pp. 1767–1784, 2019.

[23] K. L. Johnson and K. L. Johnson, *Contact Mechanics*. Cambridge, U.K.: Cambridge Univ. Press, 1987.

[24] A. Carpinteri, *Structural Mechanics: A Unified Approach*. Boca Raton, FL, USA: CRC Press, 2017.

[25] S. Balasubramanian, A. M.-Calderon, A. R.-Brami, and E. Burdet, "On the analysis of movement smoothness," *J. Neuroeng. Rehabil.*, vol. 12, no. 1, 2015, Art. no. 112.